

A new scheme for isomer pumping and depletion with high-power lasers

C.-J. Yang,¹ K. M. Spohr,^{1,2} M. Cernaianu,¹ D. Doria,¹ P. Ghenuche,¹ and V. Horný¹

¹*ELI-NP, “Horia Hulubei” National Institute for Physics and Nuclear Engineering,
30 Reactorului Street, RO-077125, Bucharest-Magurele, Romania**

²*School of Computing, Engineering and Physical Sciences,
University of the West of Scotland, High Street, PA1 2BE, Paisley, Scotland†*

(Dated: April 12, 2024)

We propose a novel scheme for the population and depletion of nuclear isomers. The scheme combines the γ -photons with energies $\gtrsim 10$ keV emitted during the interaction of a contemporary high-intensity laser pulse with a plasma and one or multiple photon beams supplied by intense lasers. Due to nonlinear effects, two- or multi-photon absorption dominates over the conventional multi-step one-photon process for an optimized gamma flash. Moreover, this nonlinear effect can be greatly enhanced with the help of externally supplied photons. These photons act such that the effective cross-section experienced by the γ -photons becomes tunable, growing with the intensity I_0 of the beam. Assuming $I_0 \sim 10^{18} \text{ Wcm}^{-2}$ for the photon beam, an effective cross-section as large as 10^{-21} cm^2 to 10^{-28} cm^2 for the γ -photon can be achieved. Thus, within state-of-the-art 10 PW laser facilities, the yields from two-photon absorption can reach 10^6 to 10^9 isomers per shot for selected states that are separated from their ground state by E2 transitions. Similar yields for transitions with higher multiplicities can be accommodated by multi-photon absorption with additional photons provided.

PACS numbers: 25.30.Bf, 21.60.Cs, 01.30.-y, 01.30.Ww, 01.30.Xx

Nuclear isomers are excited states of nuclei that have a longer half-life ($t_{1/2} \gtrsim 1$ ns) than the states in the prompt decay paths of a nucleus following an induced excitation. Isomers with $t_{1/2} > 10$ years (e.g., ^{93m}Nb , ^{113m}Cd , ^{178m}Hf , etc.) are ideal candidates for nuclear batteries that outperform conventional ones by $\times 10^6$ in energy density [1]. Many isomers with $t_{1/2} \gtrsim$ hours have proven medical potentials [2–4]. Furthermore, isomers generally serve as pathways to enable nuclear lasing [5, 6]. Since their discovery [7], the efficient creation and induced depopulation of isomers has been one of the outstanding problems in physics. Any breakthrough on this topic will enable exciting applications in nuclear photonics.

The production of isomers by brute force via photon absorption toward the desired state is inefficient and riddled with technological challenges. In general, it requires pumping through intermediate states with shorter lifetimes, except for a few cases where favorable transitions of ground-state to a higher excited state followed by its decay into the isomer state exist. Herein, the dilemma is that generating a large number of γ -photons to be absorbed resonantly by the nuclear level within a short time is difficult. Moreover, the direct pumping of a state exhibiting a longer half-life is challenged by the relatively narrow absorption bandwidth (e.g., 10 ps correspond to a natural width of only $6.6 \cdot 10^{-5}$ eV), which leads to the so-called graser dilemma, i.e., the half-life/width combinations given in nature requires elusive laser pumping powers or the very unrealistic scenario of an induced nuclear explosion [5, 6]. As the energy gap between nuclear

transitions often leads to isomers $\gtrsim 100$ keV, no existing laser can be used in direct pumping.

Other than γ -excitation, alternative ways to generate isomers discussed in the past involve various nuclear reactions or Coulomb excitation provided that suitable seed nuclei are available [8, 9]. However, the triggered depletion of isomers, i.e., how to harvest the energy with high efficiency, seems still an unsolvable problem [10–32]. Nevertheless, proposals that utilizing intensive ($\gtrsim 10^{10} \text{ Wcm}^{-2}$) optical photons toward a virtual state followed by spontaneous emissions to the desired state provide an interesting alternative [33–38].

High-power laser systems (HPLS) can become core entities to spearhead associated developments [39–51] as they are able now to deliver intensities up to $\mathcal{P} \sim 10^{21-23} \text{ Wcm}^{-2}$ [52–57]¹. When interacting with an overdense target, HPLS accelerate electrons in the materials to highly relativistic energies and drive strong currents in the plasma environment. The extreme, quasistatic magnetic fields then interact with energetic electrons, generate dense γ -photons [58–69] and rejuvenates the hope of a mass production of isomers. However, existing schemes of manipulating isomers incorporate either a single- or multi-step excitation via very dense γ -photons to some “stepping” intermediate states in the decay chain toward the desired state [27, 28, 70, 71], which, even with an optimal HPLS-based γ -production, give yield estimations that are far from even suggesting a technical realization [68, 72–80]. Reaching a sufficient population yield for the isomer population remains an insurmountable challenge.

* chieh.jen@eli-np.ro (corresponding author)

† klaus.spohr@eli-np.ro (corresponding author)

¹ See <https://www.icuil.org/> for a comprehensive overview of current facilities.

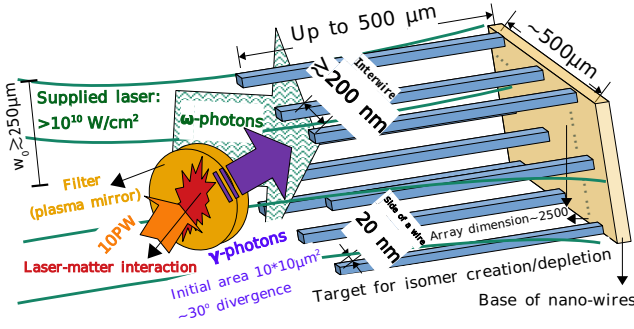


Figure 1. Schematic illustration of the proposed scheme with an optimal target design. (Dimensions not to scale, see supplemental materials for reasons behind the given parameters)

In this work, we demonstrate that the efficiency of isomer pumping and successive depletion can be drastically improved ($\geq 10^{10}$ -fold) by combining the γ -photons generated by an HPLS with intense supplied optical/infrared photons ($\equiv \omega$ -photons), through a two- or multi-photon absorption (nPA) mechanism, as illustrated in Fig. 1. This nPA mechanism prescribes a nonlinear growth of the yields [35–37, 81–84] and becomes dominating as the intensity of the incident photons grows.

Denoting E_i and I_i the energy and the corresponding intensity² of the i^{th} photon category in an nPA process. Assuming the energies are tunable so that $E \equiv \sum_{i=1}^n E_i$ equals the gap between the initial state and the state one wishes to populate, then

$$\frac{d\mathcal{Y}_{(n)}}{dz} = N \cdot (I_1 I_2 \cdot \dots \cdot I_n \sigma_{npa} + \dots), \quad (1)$$

where $\mathcal{Y}_{(n)}$ denotes the yields of the final state per unit time given by n -photon absorption, N is the number of nuclei photons encountered per distance in the target dz , and σ_{npa} is the generalized cross-section for nPA and is a function of each E_i . The unit of σ_{npa} is $[\text{length}]^{2n}[\text{time}]^{n-1}$, i.e., a direct extension to the well-known 2PA cross-section ($\sigma_{2pa} = \sigma_{GM}$)[81]. Note that nPA corresponds to iterations on the interaction Hamiltonian H_{int} —which is normally further expanded into electromagnetic multipoles. Therefore, unless the product of intensities reaches a sufficient threshold, $I_1 I_2 \cdot \dots \cdot I_n \sigma_{npa}$ is negligible compared to 1PA with an H_{int} that equals to the multipoles of the transition. Conversely, additional terms (denoted as “...” in Eq. (1)) will dominate over $I_1 I_2 \cdot \dots \cdot I_n \sigma_{npa}$ if any of the I_i satisfies

$$\sigma_{npa} < I_i \sigma_{(n+1)pa}. \quad (2)$$

In this case, two photons (instead of one) in the i^{th} category being absorbed at once will be preferred, and the

original nPA process is surpassed by a $(n+1)$ PA process. One can rewrite $I_1 I_2 \sigma_{2pa}$ as $I_1 \sigma_{eff}(I_2)$ for 2PA. Thus, the effective cross-section $\sigma_{eff}(I_2)$ experienced by those I_1 -photons becomes tunable and depends on I_2 . The dependence is linear only when I_2 is low, i.e., $\sigma_{eff}(I_2) \sim I_2 \sigma_{2pa}$, but becomes $\sim I_2^2 \sigma_{3pa}$ when I_2 reaches a critical value so that $\sigma_{2pa} < I_2 \sigma_{3pa}$. For convenience, we assume that all of the I_i in Eq. (1) are below their critical values governed by Eq. (2)³. In that case, one can define the effective cross-section experienced by I_1 (via nPA) as

$$\sigma_{eff}^{npa}(I_2, I_3, \dots, I_n) = I_2 \cdot \dots \cdot I_n \sigma_{npa}, \quad (3)$$

where the unit of σ_{eff}^{npa} is $[\text{length}]^2$. The remaining task is to estimate the size of σ_{npa} . The concept of nPA has been widely practised in atomic and molecular physics, though it has yet to be observed experimentally in nuclear systems⁴. Nevertheless, the theoretical derivation first introduced by Göppert-Mayer [81] and its later extensions [94–96] are very general and do not rely on whether the systems at hand are nuclei or atoms. Denoting e as the charge, $|i\rangle$, $|m\rangle$ and $|f\rangle$ as the initial, intermediate, and final state in the process, the transition rate of 2PA reads [97],

$$R_{2pa} = \frac{e^4 \mathcal{E}_1^2 \mathcal{E}_2^2}{16\hbar^4} |\mathcal{M}|^2 2\pi \delta_t(\omega - \omega_1 - \omega_2), \quad (4)$$

where $\omega_i = E_i/\hbar$, with E_i the energy of the i^{th} photon with amplitude \mathcal{E}_i , \hbar the reduced Planck constant. δ_t has the dimension of [time], and

$$\mathcal{M} = \sum_m \left[\frac{\langle f | \hat{H}_2 | m \rangle \langle m | \hat{H}_1 | i \rangle}{\omega_1 - \omega_{mi}} + (1 \leftrightarrow 2) \right], \quad (5)$$

where $\omega_{mi} = \omega_m - \omega_i$ is the energy gap between the initial and the m state, with m representing a physical state which belongs to any eigenstate of the nuclear Hamiltonian (including i or f itself). To maximize the transition amplitude $|\mathcal{M}|$, the virtual state after each photon absorption needs to resonate with a physical state to minimize the denominators of Eq. (17).

In the atomic case, the wavefunctions of excited-states can be calculated accurately [98–102], which enables an evaluation of $|\mathcal{M}|$ [95, 96, 103–109]. Unfortunately, most of the excited states of nuclei cannot be accurately described due to a combination of a complicated structure of nuclear forces and the difficulty in solving the nuclear many-body problem [110–113]. In this work, we do not focus on specific nuclei and adopt the Weisskopf estimates [114] to evaluate the transition operators $\langle \hat{H}_i \rangle$ due to the i^{th} photon. For convenience, we define $i = 1$ as the γ -photons and $i = 2$ as the ω -photons.

² Note that I_i is the number of photons per area per time, while $\mathcal{P}_i \equiv I_i E_i$ is the energy flux—which is later denoted as intensity in the unit of Wcm^{-2} .

³ Any exceeding I_i will be re-distributed in favor of a new category $(n+1)$, as $(n+1)$ PA dominates in this case.

⁴ Reverse processes have been observed based on double γ -decay [85–93].

We consider two cases for 2PA. Case (a) represents the situation that no intermediate state within ~ 1 keV from $\langle i \rangle$ or $\langle f \rangle$ exists. Therefore, the virtual state needs to resonate with either $\langle i \rangle$ or $\langle f \rangle$ itself, leading the denominator in Eq. (17) to become ω_2 (i.e., the one labeled as the supplied photon). The corresponding transition \hat{H}_2 must be at least M1 or higher, as $\langle m \rangle$ is represented by either $\langle i \rangle$ or $\langle f \rangle$ and the angular momentum quantum number between the transition $\Delta J^\pi = 0^{+5}$. For \hat{H}_1 , E1 gives the largest possible matrix element. Case (b) has $\langle m \rangle$ separated from $\langle i \rangle$ or $\langle f \rangle$ by $\Delta J^\pi = 1^-$ and $\Delta E \lesssim 1$ keV. In this case, each photon can undergo E1 transition.

We note that $\langle i \rangle$ and $\langle f \rangle$ can be any eigenstate of the nuclear Hamiltonian. For isomer creation, $\langle f \rangle$ is the isomer or a higher excited state that has a favorable decay path to the desired isomer, and $\langle i \rangle$ is the initial state. For depletion, $\langle i \rangle$ is the isomer and $\langle f \rangle$ is the state one wishes to arrive, which can be any excited state with J^π favorable for decaying into the ground-state.

The realistic cross-section of 2PA is conventionally expressed as [105]

$$\sigma_{2pa} = \sigma_0 g G, \quad (6)$$

with σ_0 (unit: [length]⁴) the line-shape-independent cross-section, g (unit: [time]) the line-shape function, and G the photon statistical factor [115, 116]. $G = 1$ for a single-mode laser and becomes larger in multi-mode cases. The value of g can be estimated by a Gaussian distribution with a full width at half maximum (FWHM) equal to the larger of the width ($\equiv w_>$) of $\langle f \rangle$ or the laser bandwidth.

$$g = 2\sqrt{\frac{\ln 2}{\pi}} \frac{1}{w_>} \sim \frac{0.939}{w_>}. \quad (7)$$

One can see that σ_{2pa} is weakened by $w_>$, which is dominated by recoil broadening and should not exceed 1 eV for solid targets. Using ultra-intense beams could potentially broaden $w_>$ [117] and free the nuclei in the solid target for an intensity $\gtrsim 10^{18}$ Wcm⁻².

With detailed derivations given in the supplemental materials [97], the effective cross-section (given in [cm²]) experienced by the γ -photon reads

$$\sigma_{eff}^{2pa, E1+E1} \approx 3 \cdot 10^{-51} \frac{E_\gamma}{w_>} \mathcal{P}_2 \frac{A^{4/3}}{(\Delta E)^2} G, \quad (8)$$

$$\sigma_{eff}^{2pa, M1+E1} \approx 5 \cdot 10^{-51} \frac{E_\gamma}{w_>} \mathcal{P}_2 \frac{A^{2/3}}{(E_2)^2} G, \quad (9)$$

where the superscripts $M1 + E1$ and $E1 + E1$ represent cases (a) and (b), respectively. E_γ and $w_>$ must have the same unit, \mathcal{P}_2 is the intensity of the supplied laser in Wcm⁻², $\Delta E = |E_m - E_{i/f}|$ (in eV) is the gap between

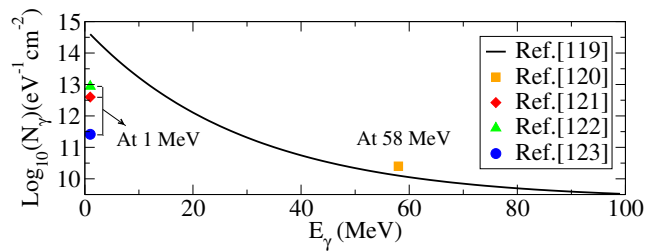


Figure 2. Number of γ -photons N_γ per eV cm² as a function of energy generated via laser-plasma interaction in a single shot converted from Refs. [119–123], with details listed in supplemental material [97]. Note that the actual γ -flux occupies an area of only $\approx 100 \mu\text{m}^2$. The accumulated time is $t \approx 15$ –50 fs.

$\langle m \rangle$ and the nearest of the initial/final state, which reduces to E_2 in the case of $M1 + E1$. A is the number of nucleons.

Eq. (8) and (9) agree with the estimates in Refs. [36, 83] if one adopts $G = 1$ and the natural width of $\langle f \rangle$ for $w_>$. However, this is likely to apply only in the cases of Mößbauer nuclei [118]. In general, $w_>$ is likely to be $10^{3\sim 4}$ times larger. Thus, the effective cross-section (10^{-26} cm² to 10^{-32} cm² for $A \approx 200$ nuclei) given before by assuming $\mathcal{P}_2 = 10^{10}$ Wcm⁻² will be suppressed accordingly. However, today's lasers can reach $\sim 10^{23}$ Wcm⁻². Therefore one can easily compensate for the $\sim 10^3$ to 10^4 suppression-factor and obtain $\sigma_{eff}^{2pa} \approx 10^{-21}$ cm² to 10^{-28} cm² with $\mathcal{P}_2 \lesssim 10^{18}$ Wcm⁻². A higher \mathcal{P}_2 , though achievable today, complicates the yield estimate, as target disintegration needs to be considered⁶.

Note that the conventional treatment of $gG \approx 1/w_>$ in Eq. (6) reduces the effective cross-section due to the assumption that the beams are near *monochromatic*. This is not the case for the γ -source generated via laser-plasma interaction, as shown in Fig. 2. Unlike any conventional beams, the spectrum distributes continuously from 1 keV to 50 MeV [119–124]. Yield estimates, in this case, require special care. The line shape of the final state does not play the same role as before, as each shifted or broaden-state will always have a combination of γ -photon plus ω -photon centered to its peak. A more convenient treatment is considering the integrated intensity of γ -photons over the energy interval equal to the total width $w_>$ of the final state. Defining such integrated intensity as ΔI_γ , as all γ -photons within that energy interval can excite the nuclei, the yield as defined in Eq. (1) becomes

$$\frac{dY_{(2)}}{dz} = N \Delta I_\gamma \frac{w_>}{\bar{w}} \sigma_{eff}^{2pa}, \quad (10)$$

⁵ Excluding the transition from $J = 0$ to $J = 0$, which is forbidden for a single photon in first order [85].

⁶ Nevertheless, this process (mechanical shock-wave propagation) is much slower than the speed of light and the nuclear transition time, so the pumping/depletion will still happen.

with $\bar{\omega}$ the bandwidth of the supplied laser.

With the γ -flash alone, photons within the narrow energy range of $E_\gamma \in [1, 1.001]$ keV reach an area density of $N_\gamma \sim 10^{12}$ cm $^{-2}$ even estimated very conservatively from Fig. 2, which corresponds to $\mathcal{P}_\gamma \approx 10^9$ Wcm $^{-2}$. Plugging \mathcal{P}_γ as \mathcal{P}_2 into Eq. (8), the effective cross-section for an incoming 1 MeV γ -photon assisted by 1 keV photons becomes⁷ $\sigma_{eff}^{2pa} \approx 10^{-37}$ cm 2 . This leads to a yield $\sim 3 \cdot 10^{-6}$ per cm in the target just by considering the combination of $E_{\gamma 1} = 1$ keV and $E_{\gamma 2} = 1$ MeV. Assuming similar N_γ persist from 1 keV to 1 MeV, then $10^6/2$ combinations are available. After summing each combination and considering the energy dependence, 10^{-4} isomers per shot are generated within 1 cm thickness in the target via 2PA. While the yields under the same condition from sequential 1PA+1PA process is 10^{-9} (assuming the cross-section at each step is 1 b, a negligible angular-divergence of γ , and an absence of favorable decay/feeding paths from higher-states). Thus, 2PA dominates over sequential photon absorption, considering only the γ -flash.

Combining the γ -photon with ω -photons supplied at $\mathcal{P} \gtrsim 10^{10}$ Wcm $^{-2}$ further increases the yields⁸, which easily reaches 10^6 per shot ($\lesssim 50$ fs). In fact, we are mainly limited by the total number of γ -photons that are actually generated per absorption width, not the ef-

fective cross-section, which is sufficiently large already for $\mathcal{P} \approx 10^{13}$ Wcm $^{-2}$ so that most of the γ 's matching the excitation energy are absorbed within 1 cm thickness in the target. Moreover, in the case of 2PA, we do not need to consider the reduction caused by the angular divergence of γ -photons as long as the whole propagation/spread stays within the target and is within the waist of the supplied laser, which is a highly desirable feature in contrast to sequential pumping.

Now, we generalize the above ingredients to enhance more transitions. First, the magnitude of the achievable σ_{eff}^{2pa} makes it possible to consider a $\langle \hat{H}_i \rangle$ of E2 type per step. A realistic E2 amplitude often exceeds the Weisskopf estimate and is only suppressed by $\sim 10^2$ relative to E1 transitions due to the collective excitation [125]. Thus, $\sigma_{eff}^{2pa, E1+E2}$ and $\sigma_{eff}^{2pa, M1+E2}$ would reach 10^{-23} cm $^2 \sim 10^{-30}$ cm 2 with \mathcal{P}_2 up to 10^{18} Wcm $^{-2}$, while M2 and higher multipolarities are further suppressed by at least 10^6 in their magnitude and are unfavorable. Second, it is straightforward to generalize 2PA to nPA, i.e., just replacing Eq. (18) by

$$R_{npa} = \frac{e^{2n} \mathcal{E}_1^2 \dots \mathcal{E}_n^2}{4^n \hbar^{2n}} |\mathcal{M}^{(n)}|^2 2\pi \delta_t(\omega - \omega_1 \dots - \omega_n), \quad (11)$$

with $\mathcal{M}^{(n)}$ as the sum over eigenstates $\langle m_2 | \sim \langle m_n |$, i.e.,

$$\mathcal{M}^{(n)} = \sum_{m_2} \dots \sum_{m_n} \left[\frac{\langle f | \hat{H}_n | m_n \rangle \dots \langle m_3 | \hat{H}_2 | m_2 \rangle \langle m_2 | \hat{H}_1 | i \rangle}{(\omega_1 - \omega_{m_2 i})(\omega_2 - \omega_{m_3 m_2}) \dots (\omega_{n-1} - \omega_{m_n m_{n-1}})} + (\text{all permutation}) \right]. \quad (12)$$

Note that, like in Eq. (17), the adopted-intermediate state $\langle m_i |$ can be the same as $\langle i |$ or $\langle f |$. Maximum resonance occurs when each virtual state is separated from an intermediate state by the natural width of the intermediate state. A favorable scenario is that each γ_i -photon (performs E1 or E2 transition) is assisted by one ω_i -photon (performs M1 transition) to reach a virtual state, i.e.,

$$\underbrace{\gamma_1 + \omega_1}_{|\Delta J| \leq E2} + \underbrace{\gamma_2 + \omega_2}_{|\Delta J| \leq E2} + \dots, \quad (13)$$

where $|\Delta J| \leq E2$ means the transition is within $|\Delta J| \in (E1, M1, E2)$. As shown in Fig. 2, the power density of the γ -photons is rather intense, i.e., $\mathcal{P}_\gamma \sim 10^9$ Wcm $^{-2}$ to 10^{12} Wcm $^{-2}$ for $E_\gamma \leq 1$ MeV. This implies

that the transition rate between nPA and 2PA will be comparable (for arbitrary large n) provided that each ω -photon beam has $\mathcal{P}_i \gtrsim 10^{16}$ Wcm $^{-2}$, $E_\omega \approx$ (width of the intermediate states), and favorable intermediate states exist. As illustrated in Fig. 3, in general, the largest contribution would be that all of the ω -photons are used in resonating with each intermediate state via M1 transitions. Each leap with $\Delta E \geq 1$ keV is completed by γ -photons from the γ -flash. Favorable intermediate states mean adjacent eigenstates $\langle m_i |$ are separated by E1, M1 or E2 transitions and with ΔE achievable by the γ -spectrum displayed in Fig. 2 (preferably ≤ 5 MeV). The total number of intermediate states is $n/2 - 1$ for nPA, with the net angular momentum difference between $\langle i |$ and $\langle f |$ up to $|\Delta J| = n$. Possible modifications to the above scheme include the scenario of the existence of adjacent intermediate states separated within reach of the energy of the ω -photons and with $|\Delta J^\pi| = 1^-$, which then favors an E1 transition for the ω -photons. Typically, an isomer separated by $|\Delta J| \gtrsim 4$ concerning all states it can decay to could already have a half-life $\gtrsim 1$ year, which would be accessible with our proposed population scheme via 4PA. Note that for isomer pumping, the J^π structure of Fig. 3 suggests that $\langle f |$ would decay easily,

⁷ Here σ_{eff}^{2pa} is further suppressed than previously estimated as ΔE or $E_2 \sim 1$ keV.

⁸ A $\gtrsim 10^3$ enhancement coming from the reduction of bandwidth from the γ -spectrum to the supplied laser, and another up to 10^6 (system-dependent) enhancement due to a smaller E_2^2 or $(\Delta E)^2$.

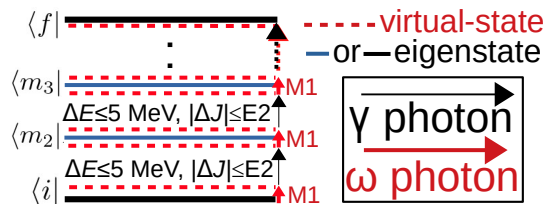


Figure 3. Illustration of an nPA scheme, where the pumping is achieved through each virtual state with gaps equal to E_{γ_i} (preferably $\lesssim 5$ MeV) or E_{ω_i} . The “:” between $\langle m_3|$ and $\langle f|$ corresponds to “...” in Eq. (13) and denotes similar pumping processes utilizing the $\gamma_i + \omega_i$ pairs. Only virtual states located around m_i contribute significantly.

so $\langle f|$ is mostly a state with favorable decay paths toward the isomer state instead of the isomer itself⁹. This feeding (through $\langle f|$) scheme also allows for an isomer population inversion against $\langle i|$. Counter-effects such as stimulated emissions or anti-Stokes processes are suppressed before the population of $\langle f|$ dominates.

Experimentally, only two photon sources are required: an ultra-short 10PW laser pulse to generate γ -photons via laser-matter interactions, the other (with $\mathcal{P} \gtrsim n \times 10^{10} \text{ Wcm}^{-2} \sim 10^{11} \text{ Wcm}^{-2}$) supplies ω -photons. Two laser sources are sufficient because each of the ω -photons will automatically select and combine with suitable γ_i -photons presented in Fig. 2 to achieve nPA. Thus, the ω_i can be the same in Eq. (13) and be supplied by one source. Using more than one ω -source is beneficial provided that it can be tuned to another energy (away from the 1st one by at least $w_{>}$), then the γ -photons in another energy interval can be utilized to increase the yields.

Our scheme applies to gas, liquid, and solid isomer targets. Depending on the shape/thickness of the target used to generate γ -photons, a filter which acts as a plasma mirror might be necessary to prevent the residue PW-pulses (after laser-matter interaction) from destroying a solid isomer-target. For solid isomer-targets, two scenarios can occur: (1) The target remains transparent for the ω -photons—which typically corresponds to non-metallic targets when $\mathcal{P} \lesssim 10^{11} - 10^{12} \text{ Wcm}^{-2}$. In this case, all photons penetrate the target and no special design is required. (2) For cases where the effect from free-electrons dominates, which corresponds to metallic targets or any highly ionized target when $\mathcal{P} \gtrsim 10^{12} \text{ Wcm}^{-2}$. In this case, the ω -photons can only penetrate within a skin depth, which is usually a few nm. To maximize the yields, we need special target designs. One possibility, as sketched in Fig. 1, is a nano-wire-like structure, which allows the laser to propagate along the surface of the wires for a longer distance, and therefore maximize the yields [79, 127–146]. The realistic waist of the γ -photons

is $\sim 5 \mu\text{m}$. One possibility to optimize the yield will be an array of square-type nano-wires, each with dimension ~ 20 nm on each side, and with a sufficient inter-wire distance ($\gtrsim 200$ nm) to allow free propagation of photons.

Note that the fascinating idea of enhancing cross-sections by supplying various intensive beams is not new [33–38, 83, 147–153]. However, we demonstrate here for the first time that the feasibility of such a mechanism can be carried out with the help of the γ -photons generated via laser-matter interaction. Therefore, we do not need to rely on any spontaneous emission coming from the anti-Stokes or Raman process, as in those previous depletion proposals. Our scheme can be applied to pump and deplete a very wide class of nuclear isomers and therefore represent a crucial step toward realizing exciting new concepts in nuclear photonics.

ACKNOWLEDGMENTS

We thank Paolo Tomassini and Bogdan Corobean for useful discussions and suggestions. This work was supported by the Extreme Light Infrastructure Nuclear Physics (ELI-NP) Phase II, a project co-financed by the Romanian Government and the European Union through the European Regional Development Fund - the Competitiveness Operational Programme (1/07.07.2016, COP, ID 1334); the Romanian Ministry of Research and Innovation: PN23210105 (Phase 2, the Program Nucleu), the ELI-RO grant Proiectul ELI12/16.10.2020 and ELI10/01.10.2020 of the Romanian Government and the IOSIN funds for research infrastructures of national interest. We acknowledge EuroHPC Joint Undertaking for awarding us access to Karolina at IT4Innovations (VŠB-TU), Czechia under project number EHPC-BEN-2023B05-023 and EHPC-REG-2023R02-006 (DD-23-83 and DD-23-157), and CINECA HPC access through PRACE-ICEI standard call 2022 (P.I. Paolo Tomassini).

SUPPLEMENTAL MATERIAL

I. DERIVATIONS OF TWO-PHOTON TRANSITION RATE

The system is perturbed by an electric field given by lasers or γ -sources consists of photons, i.e.,

$$H_{int} \equiv \vec{\mathbf{E}} = \sum_{i=1}^n \mathcal{E}_i \hat{\mathbf{e}}_i \cos[\vec{k}_i \vec{r} - \omega_i t]. \quad (14)$$

Here $|\vec{k}_i| = E_i/\hbar c$, $\omega_i = E_i/\hbar$, with E_i the energy of the i^{th} photon with amplitude \mathcal{E}_i propagates in direction $\hat{\mathbf{e}}_i$, \hbar the reduced Planck constant and c the speed of light. t is the time. In this work we will focus on the absorption case, thus keeping only the $e^{-i\omega_i t}$ component

⁹ Replacing the last step in Fig. 3 by an anti-Stokes process to reach the desired isomer state is possible and can be crucial to nuclear lasers, which will be discussed in a following work [126].

of the cosine function in Eq. (14), and we consider each single-photon transition through intermediate states is of dipole (E1 or M1) form (i.e., expanding $e^{i\vec{k}_i\vec{r}} = 1 + i\vec{k}_i\vec{r} + \dots$ in Eq. (14) and keeping the components up to $O(\vec{k}_i\vec{r})$).

$$a^{[2]}(t) = \frac{e^2 \mathcal{E}_1 \mathcal{E}_2}{4\hbar^2} \sum_m \left[\frac{\langle f | \hat{H}_2 | m \rangle \langle m | \hat{H}_1 | i \rangle e^{i(\omega - \omega_1 - \omega_2)t} - 1}{\omega_1 - \omega_{mi}} + (1 \leftrightarrow 2) \right], \quad (15)$$

with the interaction Hamiltonian

$$\begin{aligned} \hat{H}_i &= \hat{e}_i \cdot \vec{r}, & \text{for E1,} \\ &= \frac{\hbar}{2Mc} \hat{e}_i \cdot (\vec{L} + g_n \vec{S}), & \text{for M1.} \end{aligned}$$

Here M is the nucleon mass, \vec{r} , \vec{L} and \vec{S} are the spatial distance, orbital and spin angular momentum operators. g_n is the g-factor for the transition particle. The subscript in \hat{H}_i denotes that only the i^{th} component part of Eq. (14) is considered. The value $\omega = \omega_f - \omega_i$ ($\omega_{mi} = \omega_m - \omega_i$) is the energy gap between the initial and the final (intermediate) state. The term $(1 \leftrightarrow 2)$ has the same form as the first term but with 1 and 2 exchanged.

Note that here the sum over $|m\rangle$ belongs to eigenstates of the system, so that it cannot overlap with the virtual state $|\tilde{v}\rangle$ with $(E_{\tilde{v}} - E_i)/\hbar = \omega_1$ or ω_2 . Eq. (15) has the same form of time-dependence as 1PA, it then leads to

$$|a^{[2]}(t)|^2 = \frac{e^4 \mathcal{E}_1^2 \mathcal{E}_2^2}{16\hbar^4} |\mathcal{M}|^2 \frac{\sin^2[(\omega - \omega_1 - \omega_2)t/2]}{[(\omega - \omega_1 - \omega_2)/2]^2}, \quad (16)$$

with

$$\mathcal{M} = \sum_m \left[\frac{\langle f | \hat{H}_2 | m \rangle \langle m | \hat{H}_1 | i \rangle}{\omega_1 - \omega_{mi}} + (1 \leftrightarrow 2) \right]. \quad (17)$$

Using the same asymptotic form at $t \rightarrow \infty$ (as appeared in Fermi's golden rule) gives the following definition of transition rate

$$R_{2pa} = \frac{e^4 \mathcal{E}_1^2 \mathcal{E}_2^2}{16\hbar^4} |\mathcal{M}|^2 2\pi \delta_t(\omega - \omega_1 - \omega_2), \quad (18)$$

where δ_t has dimension of [time].

II. DERIVATIONS OF EFFECTIVE CROSS SECTION

With the line-shape function g given by Eq. (7) in the main text, the effective cross-section for an incoming γ -photon can be obtained by firstly replacing the δ -function in Eq. (18) by g (with \tilde{R}_{2pa} denoting this change), and

Taking out the $\vec{k}_i\vec{r}$ part and denoting e as the charge, $|i\rangle$, $|m\rangle$ and $|f\rangle$ the initial, intermediate, and final state in the transition process, the transition amplitude for 2PA can then be expressed as

then dividing \tilde{R}_{2pa} by the flux multiplied by its velocity, i.e., $I_\gamma c$. This leads to

$$\sigma_{eff}^{2pa} = \frac{\tilde{R}_{2pa}}{I_\gamma c} G. \quad (19)$$

Using the relation $4\pi I_i \omega_i = \frac{\varepsilon_0 c}{2} |\mathbf{E}_i|^2$, where I_i is the intensity of photons and \mathbf{E}_i is the i^{th} component of Eq. (14), one has

$$\sigma_{eff}^{2pa} = (2\pi)^3 \frac{e^4 \omega_1 \omega_2}{c^2 \hbar^4 \varepsilon_0^2} I_2 |\mathcal{M}|^2 g G, \quad (20)$$

where ε_0 is the vacuum permittivity. According to Weisskopf estimates (which gives reasonable matrix elements within a factor $\sim 10^2$ with respect to experiments), the matrix element $|\langle \hat{H}_i \rangle|$ in Eq. (17) has the following form¹⁰

$$|\langle \hat{H}_i \rangle| = \sqrt{B(\text{typ}, l_i)}, \quad (21)$$

with $B(\text{typ}, l_i)$ the reduced transition probabilities

$$B(E, l_i) = \frac{1}{4\pi} \left[\frac{3}{l_i + 3} \right]^2 R^{2l_i}, \quad (22)$$

$$B(M, l_i) = \frac{10}{\pi} \left[\frac{3}{l_i + 3} \right]^2 R^{2(l_i - 2)} \left(\frac{\hbar}{2Mc} \right)^2. \quad (23)$$

For dipole transition $l_i = 1$. Therefore $|\langle H_i^{E1} \rangle| \approx R/4.7$, where the radius of nucleus $R \sim r_0 A^{1/3}$ with $r_0 \approx 1.2$ [fm] and A the number of nucleons. $|\langle H_i^{M1} \rangle| \approx \frac{\sqrt{10}}{4.7} \frac{\hbar}{Mc}$.

III. DETAILS OF THE CONVERSION IN THE γ SPECTRUM

The γ spectrum given in Fig. 2 in the main text adopts data points converted from the brilliance listed in Refs. [119-123]. Note that the brilliance, B_r , is given in unit $[\text{s}^{-1} \text{mm}^{-2} \text{mrad}^{-2} (0.1\% \text{BW})^{-1}]$. Meanwhile, the crucial quantity is the flux of the photons per bandwidth

¹⁰ The index $\langle i \rangle$, $\langle f \rangle$ and $\langle m \rangle$ are dropped as the detailed wavefunction no longer matters in Weisskopf estimates.

(BW) coming out from the initial area they were generated. Nevertheless, the conversion is straightforward, provided that the duration of the γ -photons and the actual angular spread of the beam (denoted as θ here) are given. Denoting N_γ (in the unit $[\text{eV}^{-1}\text{cm}^{-2}]$) the areal density of photons accumulated within 1 eV interval at a given energy E_γ , one has

$$N_\gamma = \frac{B_r \times [\text{duration in fs}] \times [\theta \text{ in mrad}]^2}{10^{15} \times [10^{-3}E_\gamma \text{ in eV}]} 10^2. \quad (24)$$

Note that the curve in Fig. 2 is produced by an exponential fit from the data of Ref. [119] at $E_\gamma = 1, 10$ and 100 MeV. However, only at $E_\gamma = 1$ MeV, $\theta = 0.7$ [rad] is given. We have therefore assumed that the same θ applies for other energies¹¹. Thus, the black curve shown in Fig. 2 could be subjected to an uncertainty up to 10 times for $E_\gamma \gtrsim 10$ MeV in the worst scenario. Similarly, for Refs. [120-123], the value of θ is adopted whenever directly available or by interpreting its value from relevant plots (i.e., those showing the angular divergence of the beam).

IV. PRACTICAL SCENARIOS OF THE HPLS-BASED γ - AND ISOMER-PRODUCTION

To enable our isomer pumping/depletion scheme, one of the prerequisites is a high-density γ -flash, which can be given by the interaction between high-power laser pulses and matter. Although laser wakefield acceleration [154, 155] based radiation schemes [156] such as bremsstrahlung and betatron radiation are specific alternatives, shooting a high-power laser pulse onto an overdense target may be the preferred approach because of the higher yields of γ -photons per eV interval, which can reach an areal density $N_\gamma \sim 10^{12} \text{eV}^{-1}\text{cm}^{-2}$ for $E_\gamma \approx 1 \text{keV} \sim 5 \text{MeV}$, as extracted very conservatively (Ref.[119] suggests $N_\gamma \sim 10^{14} \text{eV}^{-1}\text{cm}^{-2}$ for the same interval) from Fig. 2 in the main text.

This mechanism starts with a laser pulse of a wavelength of $\lambda \sim 1 \mu\text{m}$ that is compressed through the chirped pulse amplification technique [157] into a time scale of $\sim 25 \text{fs}$ to 50fs to achieve intensities up to $\mathcal{P} \sim 10^{21} \text{Wcm}^{-2}$ to $\mathcal{P} \sim 10^{23} \text{Wcm}^{-2}$. Such an ultraintense infrared pulse then interacts with a solid target and ionizes its electrons, forming a plasma environment. Consequently, this laser-matter interaction accelerates part of the electrons to relativistic energies.

These pre-accelerated electrons then interact with the laser field, emitting the high energy radiation, typically via the non-linear Thomson or Compton scattering mechanisms. Multiple schemes for generating dense γ -photons exist and are cited as [119-123] in the main

text. In those schemes, the temporal contrast of the HPLS can significantly influence the properties of generated γ -flash. However, there are techniques to improve the contrast, as for instance the plasma mirror, although at the expense of the main pulse energy. Ref. [119] in the main text suggests a 10-fold reduction of the γ -flux if the laser power is reduced from 10 PW to 3 PW. In this scenario, the data represented in Fig. 2 of the main text can practically be rescaled accordingly.

During the generation of γ -photons, particles such as electrons, low-energy (i.e., eV-level) photons, ions, and target debris are usually produced. Although charged particles could potentially contribute to isomer pumping/depletion (e.g., via Coulomb excitation) and might be desirable, they could also destroy a solid-type isomer target. The most straightforward way to sufficiently attenuate the population of eV-level photons and charged particles, block the debris, and prevent crucial damage to the isomer target is to place a solid filter between the target of laser-matter interaction and the isomer target. As illustrated in Fig. 1 in the main text, such a filter also serves as a plasma mirror to absorb/reflect/scatter the laser light.

A filter of about 1 mm thickness or more (e.g., 1 mm Tungsten) is sufficient to stop the high population of low-energy particles, which can cause damage to the isomer target. Such a filter would still have a negligible effect in absorbing the γ -flash. However, the inclusion of such a filter will increase the distance between the γ -photon source and isomer target; hence, it is sensible to minimize its thickness using, for instance, high- Z materials.

Note that a crucial advantage of our scheme is that the ω -photons coming from the supplied laser are not required to be aligned to the γ -photons for multi-photon absorption to occur, although the spatial overlap between γ -photons, ω -photons, and the isomer target is of the essence. The beam quality of the γ -photons determines the achievable overlap. PIC simulations (Refs. [119-123]) suggest that the majority of the γ -photons are generated from an initial area $\sim 10 \mu\text{m} \times 10 \mu\text{m}$ and exhibit an angular divergence $\theta \sim 30 \text{deg}$. Therefore, the flux would be reduced by a factor ~ 2000 after propagating $\sim 1 \text{mm}$. In any case, assuming a $\sim 2000\times$ diluted γ -intensity is still remediable by the supplied ω -photons¹², the supplied laser needs to be adjusted to have a waist $w_0 \gtrsim 250 \mu\text{m}$ to cover the entire path of the γ -photons up to a distance $\approx 1 \text{mm}$. This is very achievable even with TW-class laser systems and a long focal mirror to achieve a focused beam with a large focal spot and several mm of Rayleigh length. Owing to the waist size and Rayleigh length larger than the region of laser-matter interaction, the TW laser can be placed either on the side facing the laser-matter interaction (slightly non-parallel to the direction of HPLS, as illustrated in Fig. 4 above), or on

¹¹ Normally, θ would be lower for higher energies.

¹² The divergence of γ -photons plays no role for a 2PA of $\omega + \gamma$ type, but it matters when more than one γ enters the nPA.

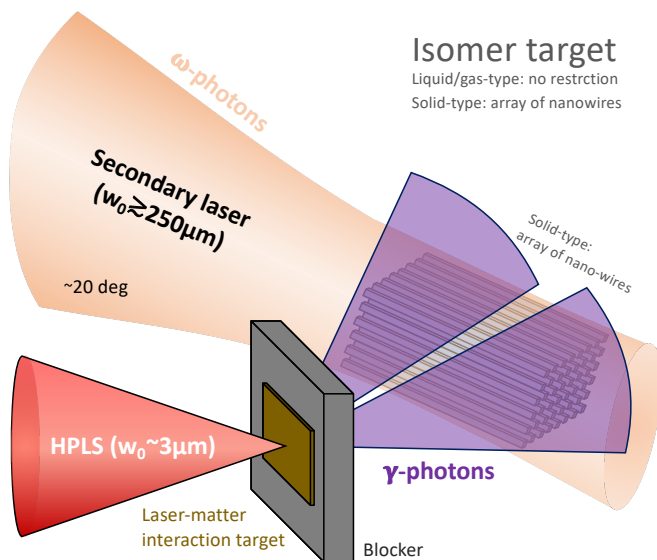


Figure 4. Illustration of an experimental setup. A γ -flash driven by the main HPLS pulse typically has two main lobes, where the isomer targets are placed correspondingly. If the isomer target is of solid form, a nano-wire-like structure is preferred (with their detailed structure illustrated in Fig. 1 of the main text), and the ω -photons need to be aligned to the nano-wires, which may be placed to have an angle ~ 20 deg with respect to the HPLS direction. If the isomer target is of gas or liquid form, all restrictions can be levitated in favoring a maximum overlap volume between the γ - and ω -photons.

the opposite side—where it is allowed to propagate anti-parallelly with respect to the HPLS¹³.

One remaining factor in the practical realization concerns the practical target design to maximize the isomer yields. As mentioned in the main text, if eV-level ω -photons are adopted, with $\mathcal{P} \gtrsim 10^{12} \text{ Wcm}^{-2}$, they can only penetrate solid targets up to a skin depth $\sim 5 \text{ nm}$. In this case, an array with a nano-wire-like structure for the isomer target is preferred. As illustrated in Fig. 1 in the main text, we estimate the dimension of each side of the nano-wire to be $\sim 20 \text{ nm}$, and an inter-wire spacing of $\gtrsim 200 \text{ nm}$. This will allow ω -photons to propagate through the entire isomer target without being blocked or reflected by the nano-wires.

Finally, it is worth noting that the above setup and restrictions regarding the isomer pumping have relevance *only* to a solid target and *only* in the case where one wishes to keep its original shape in favor of pumping/depletion with continuous cycles. In general, gas or liquid forms of isomers or a one-time-use solid target can be employed with a much simpler experimental setup.

-
- [1] M. A. Prelas, C. L. Weaver, M. L. Watermann, E. D. Lukosi, R. J. Schott, and D. A. Wisniewski, *Progress in Nuclear Energy* **75**, 117–148 (2014).
- [2] C. Nitipir, D. Niculae, C. Orlov, M. Barbu, B. Popescu, A. Popa, A. Stoian Pantea, A. Stanciu, B. Galateanu, O. Gingham, G. Papadakis, B. Izotov, D. Spandidos, A. Tsatsakis, and C. Negrei, *Oncology Letters* (2017), 10.3892/ol.2017.7141.
- [3] N. J. M. Klaassen, M. J. Arntz, A. Gil Arranja, J. Roosen, and J. F. W. Nijssen, *EJNMMI Radiopharmacy and Chemistry* **4** (2019), 10.1186/s41181-019-0066-3.
- [4] G. Sgouros, L. Bodei, M. R. McDevitt, and J. R. Nedrow, *Nature Reviews Drug Discovery* **19**, 589–608 (2020).
- [5] G. C. Baldwin, J. C. Solem, and V. I. Gol’danskii, *Rev. Mod. Phys.* **53**, 687 (1981).
- [6] G. C. Baldwin and J. C. Solem, *Rev. Mod. Phys.* **69**, 1085 (1997).
- [7] O. Hahn, *Die Naturwissenschaften* **9**, 84 (1921).
- [8] S. A. Karamian and J. J. Carroll, *Phys. Rev. C* **83**, 024604 (2011).
- [9] J. Feng, W. Wang, C. Fu, L. Chen, J. Tan, Y. Li, J. Wang, Y. Li, G. Zhang, Y. Ma, and J. Zhang, *Physical Review Letters* **128** (2022), 10.1103/physrevlett.128.052501.
- [10] C. J. Chiara, J. J. Carroll, M. P. Carpenter, J. P. Greene, D. J. Hartley, R. V. F. Janssens, G. J. Lane, J. C. Marsh, D. A. Matterns, M. Polasik, J. Rzakiewicz, D. Seweryniak, S. Zhu, S. Bottoni, A. B. Hayes, and S. A. Karamian, *Nature* **554**, 216 (2018).
- [11] S. Guo, Y. Fang, X. Zhou, and C. M. Petrache, *Nature* **594**, E1 (2021).
- [12] S. Guo, B. Ding, X. H. Zhou, Y. B. Wu, J. G. Wang, S. W. Xu, Y. D. Fang, C. M. Petrache, E. A. Lawrie, Y. H. Qiang, Y. Y. Yang, H. J. Ong, J. B. Ma, J. L. Chen, F. Fang, Y. H. Yu, B. F. Lv, F. F. Zeng, Q. B. Zeng, H. Huang, Z. H. Jia, C. X. Jia, W. Liang, Y. Li, N. W. Huang, L. J. Liu, Y. Zheng, W. Q. Zhang, A. Rohilla, Z. Bai, S. L. Jin, K. Wang, F. F. Duan, G. Yang, J. H. Li, J. H. Xu, G. S. Li, M. L. Liu, Z. Liu, Z. G. Gan, M. Wang, and Y. H. Zhang, *Phys. Rev. Lett.* **128**, 242502 (2022).
- [13] Y. Wu, C. H. Keitel, and A. Pálffy, *Phys. Rev. Lett.* **122**, 212501 (2019).
- [14] V. Goldanskii and V. Namiot, *Physics Letters B* **62**, 393 (1976).
- [15] P. Morel, *AIP Conference Proceedings* (2005), 10.1063/1.1945195.
- [16] A. Pálffy, J. Evers, and C. H. Keitel, *Phys. Rev. Lett.* **99**, 172502 (2007).

¹³ In this case, the base where nano-wires are planted will be shifted to the HPLS side and integrate with the plasma mirror.

- [17] D. Belic, C. Arlandini, J. Besserer, J. de Boer, J. J. Carroll, J. Enders, T. Hartmann, F. Käppeler, H. Kaiser, U. Kneissl, M. Loewe, H. J. Maier, H. Maser, P. Mohr, P. von Neumann-Cosel, A. Nord, H. H. Pitz, A. Richter, M. Schumann, S. Volz, and A. Zilges, *Phys. Rev. Lett.* **83**, 5242 (1999).
- [18] I. Stefanescu, G. Georgiev, F. Ames, J. Äystö, D. L. Balabanski, G. Bollen, P. A. Butler, J. Cederkäll, N. Champault, T. Davinson, A. D. Maeschalck, P. Delahaye, J. Eberth, D. Fedorov, V. N. Fedosseev, L. M. Fraile, S. Franchoo, K. Gladnishki, D. Habs, K. Heyde, M. Huyse, O. Ivanov, J. Iwanicki, J. Jolie, B. Jonsson, T. Kröll, R. Krücken, O. Kester, U. Köster, A. Lagoyannis, L. Liljeby, G. L. Bianco, B. A. Marsh, O. Niedermaier, T. Nilsson, M. Oinonen, G. Pascovici, P. Reiter, A. Saltarelli, H. Scheit, D. Schwalm, T. Sieber, N. Smirnova, J. V. D. Walle, P. V. Duppen, S. Zemlyanoi, N. Warr, D. Weisshaar, and F. Wenander, *Phys. Rev. Lett.* **98**, 122701 (2007).
- [19] O. Roig, V. Méot, B. Rossé, G. Bélier, J.-M. Daugas, A. Letourneau, A. Menelle, and P. Morel, *Phys. Rev. C* **83**, 064617 (2011).
- [20] J. J. Carroll, M. S. Litz, K. A. Netherton, S. L. Henriquez, N. R. Pereira, D. A. Burns, and S. A. Karamian, *AIP Conference Proceedings* (2013), 10.1063/1.4802396.
- [21] V. Kirischuk, V. Ageev, A. Dovbnaya, S. Kandybei, and Y. Ranyuk, *Physics Letters B* **750**, 89 (2015).
- [22] L. von der Wense, B. Seiferle, M. Laatiaoui, J. B. Neumayr, H.-J. Maier, H.-F. Wirth, C. Mokry, J. Runke, K. Eberhardt, C. E. Düllmann, N. G. Trautmann, and P. G. Thirolf, *Nature* **533**, 47 (2016).
- [23] J. Carroll, S. Karamian, R. Propri, D. Gohlke, N. Caldwell, P. Ugorowski, T. Drummond, J. Lazich, H. Roberts, M. Helba, Z. Zhong, M.-T. Tang, J.-J. Lee, and K. Liang, *Physics Letters B* **679**, 203 (2009).
- [24] J. Gunst, Y. Wu, C. H. Keitel, and A. Pálffy, *Phys. Rev. E* **97**, 063205 (2018).
- [25] Y. Wu, J. Gunst, C. H. Keitel, and A. Pálffy, *Phys. Rev. Lett.* **120**, 052504 (2018).
- [26] J. Rzadkiewicz, M. Polasik, K. Ślabkowska, L. Syrocki, J. J. Carroll, and C. J. Chiara, *Phys. Rev. Lett.* **127**, 042501 (2021).
- [27] S. Olariu and A. Olariu, *Phys. Rev. C* **58**, 333 (1998).
- [28] S. Olariu and A. Olariu, *Phys. Rev. C* **58**, 2560 (1998).
- [29] P. M. Walker, G. D. Dracoulis, and J. J. Carroll, *Phys. Rev. C* **64**, 061302(R) (2001).
- [30] E. V. Tkalya, *Phys. Rev. C* **71**, 024606 (2005).
- [31] P. Walker and G. Dracoulis, *Nature* **399**, 35 (1999).
- [32] K. M. Spohr et al., *Eur. Phys. J. A* **59**, 281 (2023).
- [33] B. Arad, S. Eliezer, and Y. Paiss, *Physics Letters A* **74**, 395 (1979).
- [34] W. Becker, R. Schlicher, and M. Scully, *Physics Letters A* **106**, 441 (1984).
- [35] S. Olariu, I. Popescu, and C. B. Collins, *Phys. Rev. C* **23**, 50 (1981).
- [36] C. B. Collins, S. Olariu, M. Petrascu, and I. Popescu, *Phys. Rev. C* **20**, 1942 (1979).
- [37] S. Olariu, I. Popescu, and C. B. Collins, *Phys. Rev. C* **23**, 1007 (1981).
- [38] W. Becker, R. R. Schlicher, and M. O. Scully, *Phys. Rev. C* **29**, 1124 (1984).
- [39] W. Wang, J. Zhou, B. Liu, and X. Wang, *Phys. Rev. Lett.* **127**, 052501 (2021).
- [40] W. Lv, H. Duan, and J. Liu, *Phys. Rev. C* **100**, 064610 (2019).
- [41] S. A. Ghinescu and D. S. Delion, *Phys. Rev. C* **101**, 044304 (2020).
- [42] L. von der Wense, P. V. Bilous, B. Seiferle, S. Stellmer, J. Weitenberg, P. G. Thirolf, A. Pálffy, and G. Kazakov, *The European Physical Journal A* **56**, 1 (2020).
- [43] X. Wang, *Phys. Rev. C* **106**, 024606 (2022).
- [44] J. J. Bekx, M. L. Lindsey, S. H. Glenzer, and K.-G. Schlesinger, *Phys. Rev. C* **105**, 054001 (2022).
- [45] J. Qi, T. Li, R. Xu, L. Fu, and X. Wang, *Phys. Rev. C* **99**, 044610 (2019).
- [46] F. Queisser and R. Schützhold, *Phys. Rev. C* **100**, 041601(R) (2019).
- [47] T. Li and X. Wang, *Journal of Physics G: Nuclear and Particle Physics* **48**, 095105 (2021).
- [48] S. Liu, H. Duan, D. Ye, and J. Liu, *Phys. Rev. C* **104**, 044614 (2021).
- [49] W. Lv, B. Wu, H. Duan, S. Liu, and J. Liu, *The European Physical Journal A* **58** (2022), 10.1140/epja/s10050-022-00697-8.
- [50] H. Xu, H. Tang, G. Wang, C. Li, B. Li, P. Cappellaro, and J. Li, *Phys. Rev. A* **108**, L021502 (2023).
- [51] Z.-W. Lu, L. Guo, Z.-Z. Li, M. Ababekri, F.-Q. Chen, C. Fu, C. Lv, R. Xu, X. Kong, Y.-F. Niu, and J.-X. Li, *Phys. Rev. Lett.* **131**, 202502 (2023).
- [52] J. W. Yoon, C. Jeon, J. Shin, S. K. Lee, H. W. Lee, I. W. Choi, H. T. Kim, J. H. Sung, and C. H. Nam, *Opt. Express* **27**, 20412 (2019).
- [53] J. W. Yoon, Y. G. Kim, I. W. Choi, J. H. Sung, H. W. Lee, S. K. Lee, and C. H. Nam, *Optica* **8**, 630 (2021).
- [54] W. Li, Z. Gan, L. Yu, C. Wang, Y. Liu, Z. Guo, L. Xu, M. Xu, Y. Hang, Y. Xu, J. Wang, P. Huang, H. Cao, B. Yao, X. Zhang, L. Chen, Y. Tang, S. Li, X. Liu, S. Li, M. He, D. Yin, X. Liang, Y. Leng, R. Li, and Z. Xu, *Opt. Lett.* **43**, 5681 (2018).
- [55] L. Yu, Y. Xu, Y. Liu, Y. Li, S. Li, Z. Liu, W. Li, F. Wu, X. Yang, Y. Yang, C. Wang, X. Lu, Y. Leng, R. Li, and Z. Xu, *Opt. Express* **26**, 2625 (2018).
- [56] C. Ur, D. Balabanski, G. Cata-Danil, S. Gales, I. Morjan, O. Tesileanu, D. Ursescu, I. Ursu, and N. Zamfir, *Nuclear Instruments and Methods in Physics Research Section B: Beam Interactions with Materials and Atoms* **355**, 198 (2015).
- [57] K. A. Tanaka, K. M. Spohr, D. L. Balabanski, S. Balascuta, L. Capponi, M. O. Cernaianu, M. Cuciuc, A. Cuciuc, I. Dancus, A. Dhal, B. Diaconescu, D. Dorra, P. Ghenuche, D. G. Ghita, S. Kisiov, V. Nastasa, J. F. Ong, F. Rotaru, D. Sangwan, P.-A. Söderström, D. Stutman, G. Suliman, O. Tesileanu, L. Tudor, N. Tsoneva, C. A. Ur, D. Ursescu, and N. V. Zamfir, *Matter and Radiation at Extremes* **5** (2020), 10.1063/1.5093535.
- [58] T. Nakamura, J. K. Koga, T. Z. Esirkepov, M. Kando, G. Korn, and S. V. Bulanov, *Phys. Rev. Lett.* **108**, 195001 (2012).
- [59] C. P. Ridgers, C. S. Brady, R. Duclous, J. G. Kirk, K. Bennett, T. D. Arber, A. P. L. Robinson, and A. R. Bell, *Phys. Rev. Lett.* **108**, 165006 (2012).
- [60] L. L. Ji, A. Pukhov, E. N. Nerush, I. Y. Kostyukov, B. F. Shen, and K. U. Akli, *Physics of Plasmas* **21**, 023109 (2014).
- [61] T. G. Blackburn, C. P. Ridgers, J. G. Kirk, and A. R.

- Bell, *Phys. Rev. Lett.* **112**, 015001 (2014).
- [62] J.-X. Li, K. Z. Hatsagortsyan, B. J. Galow, and C. H. Keitel, *Phys. Rev. Lett.* **115**, 204801 (2015).
- [63] H. X. Chang, B. Qiao, T. W. Huang, Z. Xu, C. T. Zhou, Y. Q. Gu, X. Q. Yan, M. Zepf, and X. T. He, *Scientific Reports* **7** (2017), 10.1038/srep45031.
- [64] X.-L. Zhu, M. Chen, T.-P. Yu, S.-M. Weng, L.-X. Hu, P. McKenna, and Z.-M. Sheng, *Applied Physics Letters* **112** (2018), 10.1063/1.5028555.
- [65] T. W. Huang, C. M. Kim, C. T. Zhou, M. H. Cho, K. Nakajima, C. M. Ryu, S. C. Ruan, and C. H. Nam, *New Journal of Physics* **21**, 013008 (2019).
- [66] F. Mackenroth and A. Di Piazza, *Phys. Rev. A* **83**, 032106 (2011).
- [67] A. Gonoskov, A. Bashinov, S. Bastrakov, E. Efimenko, A. Ilderton, A. Kim, M. Marklund, I. Meyerov, A. Muraviev, and A. Sergeev, *Phys. Rev. X* **7**, 041003 (2017).
- [68] J. Snyder, L. L. Ji, K. M. George, C. Willis, G. E. Cochran, R. L. Daskalova, A. Handler, T. Rubin, P. L. Poole, D. Nasir, A. Zingale, E. Chowdhury, B. F. Shen, and D. W. Schumacher, *Physics of Plasmas* **26** (2019), 10.1063/1.5087409.
- [69] X. Shen, A. Pukhov, and B. Qiao, *Communications Physics* **7** (2024), 10.1038/s42005-024-01575-z.
- [70] N. Tsoneva, C. Stoyanov, Y. P. Gangrsky, V. Y. Ponomarev, N. P. Balabanov, and A. P. Tonchev, *Phys. Rev. C* **61**, 044303 (2000).
- [71] J. Feng, Y. Li, J. Tan, W. Wang, Y. Li, X. Zhang, Y. Meng, X. Ge, F. Liu, W. Yan, C. Fu, L. Chen, and J. Zhang, *Laser & Photonics Reviews* (2023), 10.1002/lpor.202300514.
- [72] M. Borghesi, J. Fuchs, S. V. Bulanov, A. J. MacKinnon, P. K. Patel, and M. Roth, *Fusion Science and Technology* **49**, 412 (2006).
- [73] M. Roth, A. Blazevic, M. Geissel, T. Schlegel, T. E. Cowan, M. Allen, J.-C. Gauthier, P. Audebert, J. Fuchs, J. Meyer-ter Vehn, M. Hegelich, S. Karsch, and A. Pukhov, *Phys. Rev. ST Accel. Beams* **5**, 061301 (2002).
- [74] B. G. Logan, R. O. Bangerter, D. A. Callahan, M. Tabak, M. Roth, L. J. Perkins, and G. Caporaso, *Fusion science and technology* **49**, 399 (2006).
- [75] M. Roth, *Plasma Physics and Controlled Fusion* **51**, 014004 (2008).
- [76] X. F. Shen, A. Pukhov, and B. Qiao, *Phys. Rev. X* **11**, 041002 (2021).
- [77] J. Sarma, A. McIlvenny, N. Das, M. Borghesi, and A. Macchi, *New Journal of Physics* **24**, 073023 (2022).
- [78] Q. S. Wang, C. Y. Qin, H. Zhang, S. Li, A. X. Li, N. W. Wang, X. M. Lu, J. F. Li, R. J. Xu, C. Wang, X. Y. Liang, Y. X. Leng, B. F. Shen, and L. L. Ji, *Physics of Plasmas* **30** (2023), 10.1063/5.0138179.
- [79] E. Eftekhari-Zadeh, M. S. Blümcke, Z. Samsonova, R. Loetzsch, I. Uschmann, M. Zapf, C. Ronning, O. N. Rosmej, D. Kartashov, and C. Spielmann, *Physics of Plasmas* **29** (2022), 10.1063/5.0064364.
- [80] Y. Zhao, H. Lu, C. Zhou, and J. Zhu, *Matter and Radiation at Extremes* **8** (2022), 10.1063/5.0121558.
- [81] M. Göppert-Mayer, *Annalen der Physik* **401**, 273 (1931).
- [82] W. Kaiser and C. G. B. Garrett, *Phys. Rev. Lett.* **7**, 229 (1961).
- [83] C. B. Collins, S. Olariu, M. Petruscu, and I. Popescu, *Phys. Rev. Lett.* **42**, 1397 (1979).
- [84] C. B. Collins, F. W. Lee, D. M. Shemwell, B. D. DePaola, S. Olariu, and I. I. Popescu, *Journal of Applied Physics* **53**, 4645 (1982).
- [85] J. Schirmer, D. Habs, R. Kroth, N. Kwong, D. Schwalm, M. Zirnbauer, and C. Broude, *Phys. Rev. Lett.* **53**, 1897 (1984).
- [86] J. Kramp, D. Habs, R. Kroth, M. Music, J. Schirmer, D. Schwalm, and C. Broude, *Nuclear Physics A* **474**, 412–450 (1987).
- [87] S. Gorodetzky, G. Sutter, R. Armbruster, P. Chevallier, P. Mennrath, F. Scheibling, and J. Yoccoz, *Phys. Rev. Lett.* **7**, 170 (1961).
- [88] D. E. Alburger and P. D. Parker, *Physical Review* **135**, B294–B300 (1964).
- [89] P. Harihar, J. D. Ullman, and C. S. Wu, *Physical Review C* **2**, 462–467 (1970).
- [90] Y. Nakayama, *Physical Review C* **7**, 322–330 (1973).
- [91] J. C. Vanderleeden and P. S. Jastram, *Phys. Rev. C* **1**, 1025 (1970).
- [92] P. A. Söderström et al., *Nature Commun.* **11**, 3242 (2020), arXiv:2001.00554 [nucl-ex].
- [93] D. Freire-Fernández, W. Korten, R. J. Chen, S. Litvinov, Y. A. Litvinov, M. S. Sanjari, H. Weick, F. C. Akinci, H. M. Albers, M. Armstrong, A. Banerjee, K. Blaum, C. Brandau, B. A. Brown, C. G. Bruno, J. J. Carroll, X. Chen, C. J. Chiara, M. L. Cortes, S. F. Dellmann, I. Dillmann, D. Dmytriiev, O. Forstner, H. Geissel, J. Glorius, A. Görgen, M. Górská, C. J. Griffin, A. Gumberidze, S. Harayama, R. Hess, N. Hubbard, K. E. Ide, P. R. John, R. Joseph, B. Jurado, D. Kalaydjieva, K. Kanika, F. G. Kondev, P. Koseoglou, G. Kosir, C. Kozhuharov, I. Kulikov, G. Leckenby, B. Lorenz, J. Marsh, A. Mistry, A. Ozawa, N. Pietralla, Z. Podolyák, M. Polettini, M. Sguazzin, R. S. Sidhu, M. Steck, T. Stöhlker, J. A. Swartz, J. Vesic, P. M. Walker, T. Yamaguchi, and R. Zidarova, “Measurement of the isolated nuclear two-photon decay in ^{72}Ge ,” (2023), arXiv:2312.11313 [nucl-ex].
- [94] P. Lambropoulos (Academic Press, 1976) pp. 87–164.
- [95] H. Friedrich, *Theoretical Atomic Physics* (Springer International Publishing, 2017).
- [96] N. B. Delone and V. P. Krainov, *Multiphoton Processes in Atoms* (Springer Berlin Heidelberg, 2000).
- [97] “See supplemental material at [url will be inserted by publisher].”
- [98] W. Johnson, C. Lin, K. Cheng, and C. Lee, *Physica Scripta* **21**, 409 (1980).
- [99] J. C. Slater, *Physical Review* **81**, 385 (1951).
- [100] C. Froese-Fischer, T. Brage, and P. Jonsson, *Computational Atomic Structure: An MCHF Approach* (Routledge, 2019).
- [101] S. Wilson, *Computer Physics Reports* **2**, 391 (1985).
- [102] S. T. Manson, *Canadian Journal of Physics* **87**, 5 (2009).
- [103] K. Omidvar, *Phys. Rev. A* **22**, 1576 (1980).
- [104] K. Omidvar, *Phys. Rev. A* **30**, 2805(E) (1984).
- [105] R. P. Saxon and J. Eichler, *Phys. Rev. A* **34**, 199 (1986).
- [106] D. J. Bamford, L. E. Jusinski, and W. K. Bischel, *Phys. Rev. A* **34**, 185 (1986).
- [107] G. Mainfray and G. Manus, *Reports on Progress in Physics* **54**, 1333 (1991).
- [108] C. Collins and J. Carroll, *Hyperfine interactions* **107**, 3 (1997).
- [109] L. Krauss-Kodytek, W.-R. Hannes, T. Meier, C. Rup-

- pert, and M. Betz, *Phys. Rev. B* **104**, 085201 (2021).
- [110] U. van Kolck, *Front. in Phys.* **8**, 79 (2020).
- [111] C. J. Yang, *Eur. Phys. J. A* **56**, 96 (2020).
- [112] C. J. Yang, A. Ekström, C. Forssén, G. Hagen, G. Rupak, and U. van Kolck, *Eur. Phys. J. A* **59**, 233 (2023).
- [113] I. Tews et al., *Few Body Syst.* **63**, 67 (2022).
- [114] J. M. Blatt and V. F. Weisskopf, *Theoretical nuclear physics* (Springer, New York, 1952).
- [115] G. S. Agarwal, *Phys. Rev. A* **1**, 1445 (1970).
- [116] P. Zoller and P. Lambropoulos, *Journal of Physics B: Atomic and Molecular Physics* **13**, 69 (1980).
- [117] M. N. Hack and M. Hamermesh, *Il Nuovo Cimento* **19**, 546 (1961).
- [118] R. L. Mössbauer, *Zeitschrift für Physik* **151**, 124 (1958).
- [119] T. Wang, X. Ribeyre, Z. Gong, O. Jansen, E. d’Humières, D. Stutman, T. Toncian, and A. Arefiev, *Phys. Rev. Appl.* **13**, 054024 (2020).
- [120] Y.-J. Gu, O. Klimo, S. V. Bulanov, and S. Weber, *Communications Physics* **1** (2018), 10.1038/s42005-018-0095-3.
- [121] K. Xue, Z.-K. Dou, F. Wan, T.-P. Yu, W.-M. Wang, J.-R. Ren, Q. Zhao, Y.-T. Zhao, Z.-F. Xu, and J.-X. Li, *Matter and Radiation at Extremes* **5** (2020), 10.1063/5.0007734.
- [122] T. Wang, D. Blackman, K. Chin, and A. Arefiev, *Phys. Rev. E* **104**, 045206 (2021).
- [123] C. Heppel and N. Kumar, *Frontiers in Physics* **10** (2022), 10.3389/fphy.2022.987830.
- [124] M. Jirka, M. Vranic, T. Grismayer, and L. O. Silva, *New Journal of Physics* **22**, 083058 (2020).
- [125] R. F. Casten (Oxford University Press/Oxford, 2001) pp. 173–296.
- [126] C. J. Yang, K. M. Spohr, and D. Doria, “Multi-photon stimulated graser assisted by laser-plasma interactions (in preparation),”.
- [127] M. A. Purvis, V. N. Shlyaptsev, R. Hollinger, C. Bargsten, A. Pukhov, A. Prieto, Y. Wang, B. M. Luther, L. Yin, S. Wang, and J. J. Rocca, *Nature Photonics* **7**, 796–800 (2013).
- [128] C. Bargsten, R. Hollinger, M. G. Capeluto, V. Kaymak, A. Pukhov, S. Wang, A. Rockwood, Y. Wang, D. Keiss, R. Tommasini, R. London, J. Park, M. Busquet, M. Klapisch, V. N. Shlyaptsev, and J. J. Rocca, *Science Advances* **3** (2017), 10.1126/sciadv.1601558.
- [129] L. Cao, Y. Gu, Z. Zhao, L. Cao, W. Huang, W. Zhou, X. T. He, W. Yu, and M. Y. Yu, *Physics of Plasmas* **17** (2010), 10.1063/1.3360298.
- [130] Z. Samsonova, S. Höfer, T. Kämpfer, I. Uschmann, R. Röder, L. Trefflich, O. Rosmej, E. Förster, C. Ronning, D. Kartashov, and C. Spielmann, *Applied Sciences* **8**, 1728 (2018).
- [131] G. Kulcsár, D. AlMawlawi, F. W. Budnik, P. R. Herman, M. Moskovits, L. Zhao, and R. S. Marjoribanks, *Physical Review Letters* **84**, 5149–5152 (2000).
- [132] G. Cristoforetti, A. Anzalone, F. Baffigi, G. Bussolino, G. D’Arrigo, L. Fulgentini, A. Giuliotti, P. Koester, L. Labate, S. Tudisco, and L. A. Gizzi, *Plasma Physics and Controlled Fusion* **56**, 095001 (2014).
- [133] R. Hollinger, C. Bargsten, V. N. Shlyaptsev, V. Kaymak, A. Pukhov, M. G. Capeluto, S. Wang, A. Rockwood, Y. Wang, A. Townsend, A. Prieto, P. Stockton, A. Curtis, and J. J. Rocca, *Optica* **4**, 1344 (2017).
- [134] K. A. Ivanov, D. A. Gozhev, S. P. Rodichkina, S. V. Makarov, S. S. Makarov, M. A. Dubatkov, S. A. Pikuz, D. E. Presnov, A. A. Paskhalov, N. V. Eremin, A. V. Brantov, V. Y. Bychenkov, R. V. Volkov, V. Y. Timoshenko, S. I. Kudryashov, and A. B. Savel’ev, *Applied Physics B* **123** (2017), 10.1007/s00340-017-6826-4.
- [135] D. Khaghani, M. Lobet, B. Borm, L. Burr, F. Gärtner, L. Gremillet, L. Movsesyan, O. Rosmej, M. E. Toimil-Molares, F. Wagner, and P. Neumayer, *Scientific Reports* **7** (2017), 10.1038/s41598-017-11589-z.
- [136] L. A. Gizzi, G. Cristoforetti, F. Baffigi, F. Brandi, G. D’Arrigo, A. Fazzi, L. Fulgentini, D. Giove, P. Koester, L. Labate, G. Maero, D. Palla, M. Romé, M. Russo, D. Terzani, and P. Tomassini, *Physical Review Research* **2** (2020), 10.1103/physrevresearch.2.033451.
- [137] G. Cristoforetti, F. Baffigi, F. Brandi, G. D’Arrigo, A. Fazzi, L. Fulgentini, D. Giove, P. Koester, L. Labate, G. Maero, D. Palla, M. Romé, R. Russo, D. Terzani, P. Tomassini, and L. A. Gizzi, *Plasma Physics and Controlled Fusion* **62**, 114001 (2020).
- [138] D. Sarkar, P. K. Singh, G. Cristoforetti, A. Adak, G. Chatterjee, M. Shaikh, A. D. Lad, P. Londrillo, G. D’Arrigo, J. Jha, M. Krishnamurthy, L. A. Gizzi, and G. Ravindra Kumar, *APL Photonics* **2** (2017), 10.1063/1.4984906.
- [139] A. Moreau, R. Hollinger, C. Calvi, S. Wang, Y. Wang, M. G. Capeluto, A. Rockwood, A. Curtis, S. Kasdorf, V. N. Shlyaptsev, V. Kaymak, A. Pukhov, and J. J. Rocca, *Plasma Physics and Controlled Fusion* **62**, 014013 (2019).
- [140] R. Hollinger, S. Wang, Y. Wang, A. Moreau, M. G. Capeluto, H. Song, A. Rockwood, E. Bayarsaikhan, V. Kaymak, A. Pukhov, V. N. Shlyaptsev, and J. J. Rocca, *Nature Photonics* **14**, 607–611 (2020).
- [141] J. Park, R. Tommasini, R. Shepherd, R. A. London, C. Bargsten, R. Hollinger, M. G. Capeluto, V. N. Shlyaptsev, M. P. Hill, V. Kaymak, C. Baumann, A. Pukhov, D. Cloyne, R. Costa, J. Hunter, S. Maricle, J. Moody, and J. J. Rocca, *Physics of Plasmas* **28** (2021), 10.1063/5.0035174.
- [142] X. Pan, M. Šmíd, L. G. Huang, T. Kluge, V. Bagnaud, E. Brambrink, T. E. Cowan, J. Colgan, T. Ebert, D. Hartnagel, M. Hesse, J. Hornung, A. Kleinschmidt, P. Perez-Martin, A. Neukirch, K. Philipp, S. Sander, G. Schaumann, A. Tebartz, B. Zielbauer, M. Roth, and K. Falk, *Physical Review Research* **6** (2024), 10.1103/physrevresearch.6.013025.
- [143] Y.-D. Xia, D.-F. Kong, Q.-Y. He, Z. Guo, D.-J. Zhang, T. Yang, H. Cheng, Y.-Z. Li, Y. Yan, X. Liang, P. Zhu, X.-L. Xie, J.-Q. Zhu, T.-S. Li, C. Lin, W.-J. Ma, and X.-Q. Yan, *Nuclear Science and Techniques* **35** (2024), 10.1007/s41365-024-01381-w.
- [144] Y. Yang, C. Lv, W. Sun, X. Ban, Q. Liu, Z. Deng, W. Qi, G. Yang, X. Zhang, F. Wan, Z. Wang, B. Zhao, J. Li, and W. Zhou, *Frontiers in Physics* **11** (2023), 10.3389/fphy.2023.1189755.
- [145] D. Kong, G. Zhang, Y. Shou, S. Xu, Z. Mei, Z. Cao, Z. Pan, P. Wang, G. Qi, Y. Lou, Z. Ma, H. Lan, W. Wang, Y. Li, P. Rubovic, M. Veselsky, A. Bonasera, J. Zhao, Y. Geng, Y. Zhao, C. Fu, W. Luo, Y. Ma, X. Yan, and W. Ma, *Matter and Radiation at Extremes* **7** (2022), 10.1063/5.0120845.
- [146] Y. Chao, L. Cao, C. Zheng, Z. Liu, and X. He, *Applied Sciences* **12**, 1153 (2022).

- [147] R. A. Müller, A. V. Volotka, and A. Surzhykov, *Phys. Rev. A* **99**, 042517 (2019).
- [148] B. Ishkhanov and I. Piskarev, *Yadernaya Fizika* **32**, 593 (1980).
- [149] E. V. Baklanov and V. P. Chebotaev, *Soviet Journal of Quantum Electronics* **6**, 345 (1976).
- [150] F. Winterberg, *AIP Conference Proceedings* (1986), [10.1063/1.35822](https://doi.org/10.1063/1.35822).
- [151] S. Eliezer, J. Martinez-Val, Y. Paiss, and G. Velarde, *Quantum Electronics* **25**, 1106 (1995).
- [152] S. Eliezer, J. Martinezval, and J. Borowitz, *Laser Physics* **5**, 323 (1995).
- [153] L. A. Rivlin, *Quantum Electronics* **34**, 23 (2004).
- [154] T. Tajima and J. M. Dawson, *Phys. Rev. Lett.* **43**, 267 (1979).
- [155] E. Esarey, C. B. Schroeder, and W. P. Leemans, *Rev. Mod. Phys.* **81**, 1229 (2009).
- [156] F. Albert and A. G. R. Thomas, *Plasma Physics and Controlled Fusion* **58**, 103001 (2016).
- [157] D. Strickland and G. Mourou, *Optics Communications* **55**, 447–449 (1985).